TITLE: Assessing pathological changes within the nucleus ambiguus of horses with Recurrent Laryngeal Neuropathy: an extreme, length-dependent axonopathy

AUTHORS: Draper, A C E; Cahalan, S D; Goodwin, D; Perkins, J D M; Piercy, R J

JOURNAL: MUSCLE & NERVE

PUBLISHER: Wiley

PUBLICATION DATE: 3 September 2019

DOI: https://doi.org/10.1002/mus.26699

Assessing pathological changes within the nucleus ambiguus of horses with Recurrent Laryngeal Neuropathy: an extreme, length-dependent axonopathy

Alexandra CE Draper BVetMed PhD,[1] Stephen Cahalan, MVB[1] David Goodwin, BSc,[1] Justin Perkins, BVetMed MS,[1] and Richard J Piercy MA VetMB PhD[1].

1: Comparative Neuromuscular Disease Laboratory, Department of Clinical Sciences and Services, Royal Veterinary College, University of London, London, UK

Acknowledgements: Alex Draper's PhD was funded by a grant received from the Horserace Betting Levy Board (no:RS251). This manuscript was authorised by the RVC for publication (CSS_01997).

Author to whom reprints are to be directed, address and email: Richard Piercy, Comparative Neuromuscular Disease Laboratory, Department of Clinical Sciences and Services, Royal Veterinary College, 4 Royal College Street, Camden, London, NW1 0TU UK
rpiercy@rvc.ac.uk

Running title: RLN Cell Body Pathology (30 spaces maximum)

We confirm that we have read the Journal's position on issues involved in ethical publication and affirm that this report is consistent with those guidelines.

None of the authors has any conflict of interest to disclose.

Assessing pathological changes within the nucleus ambiguus of horses with recurrent laryngeal neuropathy: an extreme, length-dependent axonopathy

Abstract:

Introduction: Equine recurrent laryngeal neuropathy (RLN) is a naturally occurring model of length-dependent axonopathy characterised by asymmetrical degeneration of recurrent laryngeal nerve axons (RLn). Distal RLn degeneration is marked, however it is unclear whether degeneration extends to include cell bodies (consistent with a neuronopathy).

Methods: With examiners blinded to RLN severity, brainstem location and side, we examined correlations between RLN severity (assessed using left distal RLn myelinated axon count) and histopathological features (including chromatolysis and glial responses) in the nucleus ambiguus cell bodies, and myelinated axon count of the right distal RLn of 16 horses.

Results: RLN severity was not associated with RLn cell body number ($p>0.05$), or degeneration. A positive correlation between the left and right distal RLn myelinated axon counts was identified ($R^2=0.57$, $p<0.05$).

Discussion: We confirm that RLN, a length-dependent distal axonopathy, occurs in the absence of detectable neuronopathy.

Key words: distal axonopathy, length-dependent axonopathy, recurrent laryngeal nerve, neuropathy, neuronopathy, horse,

Introduction

Length-dependent axonopathies represent a large group of neurological diseases characterised by degeneration of long (sensory and motor) nerves with genetic and acquired causes [1-4]. Although these examples of length-dependent axonopathies have diverse aetiologies, it has been hypothesised that many of them share similar pathogeneses, such as axonal transport deficits, cytoskeletal dysfunction or metabolic imbalances that are ultimately catastrophic to these axons due to their extreme length[5]. Large animal models are crucial for the development of effective treatment options, as they recapitulate the length of the affected nerves. Indeed, large animal models of human disease are increasingly recognised as important, as significant differences become apparent between human diseases and their rodent models[6].

Equine RLN is an asymmetrical, primarily distal axonopathy affecting the recurrent laryngeal nerves (RLn) (left more so than the right). These nerves are the longest motor nerves in the horse (in tall horses the left RLn can be 2.5m in length and it is up to 30cm longer than the right RLn[7]). The disease is characterised by neurogenic atrophy and paresis of the intrinsic laryngeal muscles[8, 9]. Despite the prevalence of RLN being as high as 42%,[10] its aetiopathogenesis is unknown; environmental and genetic factors likely interplay to produce the RLN-phenotype[11-13].

There is extensive characterisation of peripheral nerve and muscle pathology in RLN[14, 15] but the presence or absence of an associated neuronopathy (i.e. a cell body reaction) within the nucleus ambiguus (which comprises the RLn's axonal cell bodies, see Supplementary Figure 1), is questionable [16-18]. In the few studies examining an accompanying

presence of neuronopathy in RLN, there were no detectable associated somal reactions or apparent loss of cell bodies within the nucleus ambiguus[16-18]. However, these investigations were hampered by unblinded analyses, possible phenotyping inaccuracies (a single laryngoscopic examination used to grade RLN severity[14, 19]) and un-matched control groups

In humans, distal axonopathies without associated cell body reactions primarily target the axon and include certain chemotherapy-induced (microtubule targeting drugs)[20], diabetic[21] and immune-mediated neuropathies (e.g. with hepatitis C virus whereby immune-mediated axonal destruction is a sequel to infection)[22]. In contrast, neurodegenerative diseases that result in both axon and cell body loss, such as amyotrophic lateral sclerosis (ALS), commonly result from the toxic effects of mutant protein aggregation or from mutations within genes that affect cell body health[23, 24]. Thus, if RLN could be definitely shown to be a distal axonopathy either with or without a neuronopathy then its application as a large animal model of human disease could be substantially supported whilst also benefitting affected horses by advancing the understanding of possible underlying aetiologies.

Here we investigate the central nervous system involvement in this equine neurological condition with a view to promoting its application in length-dependent motor axonopathy research. We investigated two hypotheses: (1) Horses with a more severe RLN phenotype (i.e low myelinated axon count in the left recurrent laryngeal nerve) show degeneration and have fewer cell bodies in their nuclei ambigui compared to horses with a less severe RLN phenotype and (2) these changes will be more pronounced in the left nucleus ambiguus compared to the right.

Methods

Subjects

Tissues were collected from 16 thoroughbred/warmblood-type male horses; all were greater than 5 years of age and had a wither height exceeding 166cm. The brainstem and distal left and right RLns (within 10cm of the larynx) were harvested from all horses. Twelve horses were obtained from an abattoir and the remaining 4, were euthanized whilst under general anaesthesia as part of a concurrent RLN study. The study was approved by the College's Clinical Research Ethical Review Board (2015 1381).

Tissue Preparation, Fixation and Sectioning

Each brainstem was placed in 4% buffered paraformaldehyde (PFA) for a minimum of 7 days and then cut transversely into four 4mm segments, due to the diffuse nature of the nucleus ambiguus: 1) 8mm rostral to the obex (R8), 2) 4mm rostral to the obex (R4), 3) at the level of the obex (R0) and 4) 4mm caudal to the obex (C4)[25]. The brainstem was placed with its rostral aspect downwards (furthest from the lid) into a fixation cassette ready for processing, with a tissue marker on the right dorsal aspect. Following processing, serial 4μm (10μm for the Luxol Fast Blue stained sections) sections were obtained and stored at room temperature prior to staining.

Following the brainstem acquisition, larynges were harvested and 2-3cm sections of both right and left recurrent laryngeal nerves were removed immediately caudal to the larynx. A distal sampling site was selected as this demonstrates the greatest pathological changes

when examining nerves by light microscopy[8, 26-30]. The nerves were secured at physiological length on a piece of cardboard to straighten the nerve fibres and the proximal end of each nerve marked. The nerves were fixed in 10% buffered PFA for approximately 2 months. After fixation, nerves were processed to resin as previously described[31]. Semi-thin sections (1µm) were cut with glass knives on an ultramicrotome (Leica OMU4) and mounted on glass slides.

Histology

The localisation of each nucleus ambiguus was performed based upon its position relative to other anatomical landmarks. Briefly, the large polygonal cell bodies of the RLns are located in the ventrolateral medulla oblongata with their highest density being found approximately 8mm rostral and caudal to the obex[25, 32]. The nuclei's borders include: axially, the radices of cranial nerve XII; abaxially, the nucleus of the spinal tract of cranial nerve V; ventrally, the lateral reticular nucleus and dorsally, the vagal nerve fibres[25, 32] (Supplementary Figure 1).

Specific stains were chosen to identify common pathological features (recorded on a continuous scale of how many cell body profiles were affected or as a dichotomous result) associated with central nervous system degeneration[33]; cell body profile numbers, chromatolysis, nuclear margination or fragmentation, a shrunken or swollen cell body profile, presence of axonal spheroids, vacuolation (present or absent), inclusion bodies, demyelination or a glial response (present or absent) were all assessed. Sequential brainstem sections were stained with hematoxylin and eosin (H&E), luxol fast blue (LFB), and cresyl violet (CV); astrocytes were identified by immunohistochemical labelling of glial fibrillary

acidic protein (GFAP)[34]. Slides were first dewaxed in xylene for at least 20 minutes at room temperature, before being rehydrated through a graded series of alcohols (100%, 100%, 90%, and 70%) and finally placed in Tris-buffered saline (TBS) for 5 minutes, and then treated with 3% hydrogen peroxide (in methanol) for 15 minutes, at room temperature, before being rinsed in TBS. Blocking with 10% goat serum in TBS was performed, for 60 minutes. The serum was removed and the primary antibody (1:200) (GFAP Ab190288 (mouse monoclonal) Abcam, UK) diluted in TBS was applied, and incubated overnight at 4^0C. A no-primary-antibody negative control was included in each batch. Three washes with TBS followed, before the application of the biotin-conjugated secondary antibody (1:500) (goat anti-mouse antibody I1903-25T-USB Stratech Scientific Labs) for 1 hour at room temperature before another wash. Streptavidin (Vectastain Elite ABC Peroxidase Kit, Vector Labs) was diluted according to the manufacturer's instructions and applied to the slides for 30 minutes at room temperature, followed by washing. DAB (3,3 diaminobenzadine) was applied to each slide for 5 minutes at room temperature, then washed with distilled water, and the sections dehydrated through a graded series of ethanols. Lastly the slides were placed in xylene for 10 minutes, and the coverslip applied using DPX (DPX Mountant for histology 06522, Sigma-Aldrich, UK). All staining was performed in sets with each brainstem level for every horse stained simultaneously to reduce any batch-effect when analyzing the sections. Semithin sections of the RLns were stained with 1% methylene blue (in distilled water) as previously described [35].

Image Analysis

Each slide was digitalised using a commercial service (IQPath Laboratory Digitalisation Service, UCL, UK). The cell bodies within the nucleus ambiguus were identified in each section (or recorded as absent), as described above, and an image captured of both the left and right-sided nuclei separately. These images were then assigned a random number to blind the horse number and side from the examiner. The number of cell bodies within the nucleus ambiguus were recorded per region, per side in all H&E images.

Recurrent Laryngeal Nerve Myelinated Axon Counts

Images of every fascicle for the entire transversely sectioned left and right RLn were captured at 40x magnification (Nikon Eclipse 50i microscope with a Leica camera), with the examiner blinded to the side and horse. For each nerve fascicle the total number of myelinated axons was automatically counted using a custom designed programme in Volocity 6.0 (PerkinElmir, NY, U.S.A). The myelinated axon count for the left RLn for each horse was used to estimate the RLN severity; i.e. horses with a lower myelinated axon count were considered to have more severe RLN.

Statistical Analysis

The total number of cell body profiles in the left nucleus ambiguus compared to the right was analysed using a two-tailed paired T-test. Differences in the total number of cell bodies present at each region, between each region and between each side (left and right nucleus ambiguus) were investigated using a two-way repeated measures ANOVA, with post-hoc (Tukey's) testing. The associations between the number of cell body profiles and the

pathological features recorded, in every region for both sides and RLN severity was assessed by linear regression. All analyses were performed in the statistical package R, and differences were considered statistically significant when $p<0.05$.

Results

Ratio of Left to Right Myelinated Axon Counts in the Recurrent Laryngeal Nerve

There was a statistically significant, and strong relationship between the myelinated axon counts in the left and right recurrent laryngeal nerves, such that as the axon count in the left nerve decreased so did the count in the right (n=14) (R^2=0.57; p=0.001) (Supplementary Figure 2).

Cell Body Numbers

The nucleus ambiguus could be identified in all horses (n=16), where tissue was present for that region. There was no significant difference between the number of cell bodies counted between the left and right nucleus ambiguus at any region, nor when the regional data was grouped (Figure 1) independent of RLN severity.

RLN Severity

RLN severity was not associated with any of the following, for any region on either the left or right side: number of cell bodies, chromatolysis, nuclear margination or fragmentation, shrunken cell body profile, swollen cell body profile, axonal spheroids, vacuolation, inclusion bodies, demyelination (Figure 3), glial response, or astrocytosis (GFAP) (Supplementary Table 1). Indeed, no vacuolation, inclusion bodies, or demyelination were identified in any horse. Examples of a typical cell body within the nucleus ambiguus (H&E and CV) and astrocytosis are presented in Figures 2 and 4.

Discussion

Here we showed a lack of detectable degeneration within or loss of RLn cell bodies, in either the left or right sides, of horses with RLN. However, it is possible that horses might not have been sampled during a period of active neurodegeneration. Cell body chromatolysis (cytoplasmic eosinophilia, loss of Nissl substance, pyknosis and eventual karyorrhexis), reactive astrocytosis, and microgliosis are the histopathological hallmarks of active neurodegeneration[36]. In rodent models, chromatolysis occurs within 48 hours of an axonal insult and lasts for 15-20 days; at this point, the cell body can regenerate if the insult has stopped or it will eventually die (taking up to 80 additional days[33]). With the latter scenario leading to a reduction in cell body numbers and, potentially the generation of a glial scar. Despite the chronic severe axonal pathology present in some of our cases, there was no evidence of glial scarring, and no association between RLN severity and cell body counts was detected; this suggests that axonal degeneration-mediated neuronal pathology is not a feature of RLN. Consequently, from our data we reject both hypotheses: RLN severity was not associated with cell body degeneration, reduced cell body numbers or demyelination in the central nervous system.

Our findings - that RLN is not associated with the RLn cell body degeneration - recapitulates the findings of other authors[17, 18, 25], and presents the novel result that RLN severity is also not associated with a reduction in nucleus ambiguus cell body number. Whilst the cell bodies associated with cranial nerves IX and XI can contribute to the cell body profiles identified in the NA, within the horse, these nerves' cell bodies cluster at the rostral and caudal regions of the NA (>8mm rostral to and >6mm caudal to the obex)[25] rather than

the majority of regions analysed here, such that we believe they had limited contribution to the cell body profiles numbers recorded. Our data is derived from a large sample size, ensuring the results were free from bias (blinding) and by using a continuous scale for RLN severity to phenotype individuals that prevents misclassification of disease status: when using laryngoscopy to phenotype horses for RLN, daily variations in applied grades can cause horses to be classified as a control, subclinical or clinical cases incorrectly[19]. Further, the extensive fibre type grouping that occurs in intrinsic laryngeal muscles supplied by diseased RLns in affected horses, very likely means that clinical phenotyping (using for example, resting or exercising laryngoscopy) is inaccurate[14].

RLN can now be classified as a distal axonopathy, without an associated degeneration of the cell bodies of the RLns[14]. The advantage of a more specific classification is that it focuses the list of likely aetiological mechanisms. In humans, distal axonopathies without the presence of a neuronopathy are seen in some forms of chemotherapy-induced neuropathy (those targeting microtubules), diabetic neuropathies (specifically distal symmetrical polyneuropathy and small fibre neuropathy), and immune-mediated axonopathies (typically occurring secondarily to infectious conditions (e.g. HIV or Campylobacter)[20-22, 37]. In these disorders, the predilection for axonal degeneration over other neuronal components is caused by diverse, but likely interrelated, perturbations to axonal transportation[38], mitochondrial functionality[39], oxidative homeostasis[40], oxygen delivery[41] and immune-mediated axonal destruction[42, 43]. In chemotherapy-induced neuropathies, microtubule-destabilizing drugs cause dismantling of the axonal cytoskeleton, which prevents normal axonal transportation[38]. This, in turn, reduces shuttling of neurotrophins, and hinders removal of aged or

dysfunctional mitochondria, potentially leading to increases in oxidative stress and reduced ATP production. Axonal transportation deficits are associated with paranodal evaginations seen by electron microscopy in RLn sections of RLN-affected horses[44]. Ischaemic lesions[28] and an infectious aetiology[45] have also been proposed by authors to cause RLN; further, the potential mechanisms underlying these diseases might be mirrored in human diabetic neuropathies (in which hyperglycaemia and ischaemia are postulated to induce the axonopathy) or immune-mediated neuropathies (in which neuronal proteins are targeted by the patient's own immune system).

Some authors have speculated that chemotherapy-induced neuropathy and diabetic neuropathies cause distal axonopathy via a final common pathway, in which Wallerian degeneration occurs in the distal axon, but the cell body is spared[37]. Wallerian degeneration is the process of systematic dismantling of an axon distal to the site of injury, via calpain activation, that results from increased axonal calcium influx, ultimately leading to orderly degradation of the cytoskeleton and membrane proteins[46]. The exact components of this common pathway have not been fully unravelled, however crucial events include the activation of the protein SARM1, and down-regulation of the NAD+ generating enzyme NMNAT2[47-49]. The overexpression of NMNAT2, in an experimental Wallerian degeneration model, delays axonal degeneration[50, 51]. These could be important proteins to investigate in the aetiopathogenesis of RLN, and other length-dependent axonopathies of humans.

The presence of reactive astrocytes in this study, in the absence of clear neuropathological changes, likely reflects regional differences in the binding of the GFAP antibody. This might reflect true differences in astrocyte activation, but can occur because of

fixation artefacts[52]. If true acute astrocytosis was present, other indicators of inflammation should have been detectable and reactive astrocytes in the form of gemistocytes might have been identified[53]. This increase in GFAP staining was not associated with RLN severity and thus its overall significance is unknown.

A finding in this study was the positive correlation between the left and right RLn myelinated axon counts. This suggests that degeneration of the left and right nerve myelinated axons occurs simultaneously, albeit to a greater extent in the left nerve. The ratio of the left:right myelinated axon counts were less than 1 in all individuals (n=14), highlighting that the left sided degeneration is most prominent even in mildly affected horses. This supports the bilateral nature of this disease process[8, 18, 26, 30, 54]. Similar, but less severe signs of this distal axonopathy have been reported to occur in the right distal nerve in RLN-affected horses with one author commenting that the degree of pathology seen in the distal right nerve [in severe RLN cases] is similar to that in the proximal left nerve[26].

The main assumption applied to this data is that the proportion of myelinated axons between the left and right RLns in horses is typically similar. In 9 young horses (<2 years old and lacking neurogenic atrophy of the laryngeal muscles) the total myelinated axon counts in the left and right distal RLns were approximately equal[27]. However, the myelinated fibre density (fibres/mm^2) of the distal left nerve was less than that of the distal right nerve in horses with subclinical RLN[54]. In line with the clinical signs of RLN being confined to the left side only, the axonal loss in this study was always more severe in the left nerve compared to the right: the lowest myelinated axon count being 27 in the left nerve, and correspondingly,

552 in the right. This further suggests that although both nerves degenerate distally, the right is less severely affected, likely because of its shorter length[7].

In conclusion, this research has confirmed that RLN occurs without evidence of cell body degeneration and has revealed an association between left and right RLn myelinated axon counts. Length-dependent axonopathies are often hard to recapitulate in rodent models: this study, and others before it, confirm that this naturally-occurring, length-dependent axonopathy of horses might be a very useful, and highly prevalent model of related diseases in humans. Future work should be directed at examining the pathophysiology of the disorder, to determine mechanisms that are shared with length-dependent axonopathies of other species in the hope of establishing new therapeutics for these disorders.

Abbreviations:

ALS Amyotrophic Lateral Sclerosis

CMT Charcot Marie Tooth disease

CV Cresyl Violet staining

GFAP Glial fibrillary acidic protein

H&E Haematoxylin and Eosin staining

LFB Luxol Fast Blue staining

NMNAT2 Nicotinamide mononucleotide adenyltransferase 2

RLN Recurrent Laryngeal Neuropathy

RLn Recurrent laryngeal nerve

SARM1 Sterile alpha and TIR motif-containing protein 1

References:

1. Kazamel, M. and P.J. Dyck, *Sensory manifestations of diabetic neuropathies: anatomical and clinical correlations.* Prosthet Orthot Int, 2015. **39**(1): p. 7-16.

2. Pareyson, D. and C. Marchesi, *Diagnosis, natural history, and management of Charcot-Marie-Tooth disease.* Lancet Neurol, 2009. **8**(7): p. 654-67.

3. Rossor, A.M., M.R. Evans, and M.M. Reilly, *A practical approach to the genetic neuropathies.* Pract Neurol, 2015. **15**(3): p. 187-98.

4. Zuchner, S., I.V. Mersiyanova, M. Muglia, N. Bissar-Tadmouri, J. Rochelle, et al., *Mutations in the mitochondrial GTPase mitofusin 2 cause Charcot-Marie-Tooth neuropathy type 2A.* Nat Genet, 2004. **36**(5): p. 449-51.

5. Prior, R., L. Van Helleputte, V. Benoy, and L. Van Den Bosch, *Defective axonal transport: A common pathological mechanism in inherited and acquired peripheral neuropathies.* Neurobiol Dis, 2017. **105**: p. 300-320.

6. Whitelaw, C.B., T.P. Sheets, S.G. Lillico, and B.P. Telugu, *Engineering large animal models of human disease.* J Pathol, 2016. **238**(2): p. 247-56.

7. Duncan, I.D. and I.R. Griffiths, *Pathological changes in equine laryngeal muscles and nerves.* Proc. 19th Ann. Conv. Amer. Assn. Equine Pract., 1973: p. 97-223.

8. Hahn, C.N., K. Matiasek, P.M. Dixon, V. Molony, K. Rodenacker, et al., *Histological and ultrastructural evidence that recurrent laryngeal neuropathy is a bilateral mononeuropathy limited to recurrent laryngeal nerves.* Equine Vet J, 2008. **40**(7): p. 666-72.

9. Rossignol, F., O. Brandenberger, J.D. Perkins, J.P. Marie, C. Mespoulhes-Riviere, et al., *Modified first or second cervical nerve transplantation technique for the treatment of recurrent laryngeal neuropathy in horses.* Equine Vet J, 2018. **50**(4): p. 457-464.

10. Brakenhoff, J.E., S.J. Holcombe, J.G. Hauptman, H.K. Smith, F.A. Nickels, et al., *The prevalence of laryngeal disease in a large population of competition draft horses.* Vet Surg, 2006. **35**(6): p. 579-83.

11. Boyko, A.R., S.A. Brooks, A. Behan-Braman, M. Castelhano, E. Corey, et al., *Genomic analysis establishes correlation between growth and laryngeal neuropathy in Thoroughbreds.* BMC Genomics,
2014. **15**: p. 259.

12. Dupuis, M.C., Z. Zhang, T. Druet, J.M. Denoix, C. Charlier, et al., *Results of a haplotype-based GWAS for recurrent laryngeal neuropathy in the horse.* Mamm Genome, 2011. **22**(9-10): p. 613-20.

13. Dupuis, M.C., Z. Zhang, K. Durkin, C. Charlier, P. Lekeux, et al., *Detection of copy number variants in the horse genome and examination of their association with recurrent laryngeal neuropathy.* Anim Genet, 2013. **44**(2): p. 206-8.

14. Draper, A.C.E. and R.J. Piercy, *Pathological classification of equine recurrent laryngeal neuropathy.* J Vet Intern Med, 2018. **32**(4): p. 1397-1409.

15. Rhee, H.S., C.M. Steel, F.J. Derksen, N.E. Robinson, and J.F. Hoh, *Immunohistochemical analysis of laryngeal muscles in normal horses and horses with subclinical recurrent laryngeal neuropathy.* J Histochem Cytochem, 2009. **57**(8): p. 787-800.

16. Cahill, J.I. and B.E. Goulden, *Further evidence for a central nervous system component in equine laryngeal hemiplegia.* N Z Vet J, 1989. **37**(3): p. 89-90.

17. Cahill, J.I. and B.E. Goulden, *Equine laryngeal hemiplegia. Part V. Central nervous system pathology.* N Z Vet J, 1986E. **34**(11): p. 191-3.

18. Duncan, I.D., *The pathology of equine laryngeal hemiplegia*. 1975, University of Glasgow: United Kingdom.

19. Perkins, J.D., R.O. Salz, J. Schumacher, L. Livesey, R.J. Piercy, et al., *Variability of resting endoscopic grading for assessment of recurrent laryngeal neuropathy in horses.* Equine Vet J, 2009. **41**(4): p. 342-6.

20. Ja'afer, F.M., F.B. Hamdan, and F.H. Mohammed, *Vincristine-induced neuropathy in rat: electrophysiological and histological study.* Exp Brain Res, 2006. **173**(2): p. 334-45.

21. Tracy, J.A. and P.J. Dyck, *The spectrum of diabetic neuropathies.* Phys Med Rehabil Clin N Am, 2008. **19**(1): p. 1-26, v.

22. Nemni, R., L. Sanvito, A. Quattrini, G. Santuccio, M. Camerlingo, et al., *Peripheral neuropathy in hepatitis C virus infection with and without cryoglobulinaemia.* J Neurol Neurosurg Psychiatry,
2003. **74**(9): p. 1267-71.

23. Bruijn, L.I., M.K. Houseweart, S. Kato, K.L. Anderson, S.D. Anderson, et al., *Aggregation and motor neuron toxicity of an ALS-linked SOD1 mutant independent from wild-type SOD1*. Science,
1998. **281**(5384): p. 1851-4.

24. Chou, S.M., *Neuropathology of amyotrophic lateral sclerosis: new perspectives on an old disease.* J Formos Med Assoc, 1997. **96**(7): p. 488-98.

25. Hackett, S.M., *The equine nucleus ambiguus: Myotopic and neurotopic representations of motor and sensory components of the recurrent laryngeal nerve.* 2000, Cornell University: Ithaca, NY, USA.

26. Cahill, J.I. and B.E. Goulden, *Equine laryngeal hemiplegia. Part I. A light microscopic study of peripheral nerves.* N Z Vet J, 1986A. **34**(10): p. 161-9.

27. Lopez-Plana, C., J.Y. Sautet, and J. Ruberte, *Muscular pathology in equine laryngeal neuropathy.* Equine Vet J, 1993. **25**(6): p. 510-3.

28. Duncan, I.D., I.R. Griffiths, and R.E. Madrid, *A light and electron microscopic study of the neuropathy of equine idiopathic laryngeal hemiplegia.* Neuropathol Appl Neurobiol, 1978. **4**(6): p. 483-501.

29. Cahill, J.I. and B.E. Goulden, *Equine laryngeal hemiplegia. Part III. A teased fibre study of peripheral nerves.* N Z Vet J, 1986C. **34**(11): p. 181-5.

30. Cahill, J.I. and B.E. Goulden, *Equine laryngeal hemiplegia. Part II. An electron microscopic study of peripheral nerves.* N Z Vet J, 1986B. **34**(10): p. 170-5.

31. Aparicio, S.R. and P. Marsden, *Application of standard micro-anatomical staining methods to epoxy resin-embedded sections.* J Clin Pathol, 1969A. **22**(5): p. 589-92.

32. de Lahunta, A.a.G., E., *Upper Motor Neuron*, in *Veterinary Neuroanatomy and Clinical Neurology*, A.a.G. de Lahunta, E., Editor. 2008, Saunders Elsevier: St Louis, Missouri, USA. p. 192-220.

33. Vinters, H.V.K.-D., B.K., *General Pathology of the Central Nervous System*, in *Greenfield's Neuropathology*, S.L. Love, D.N.; Ellison, D.W., Editor. 2008, Hodder Arnold: Boca Raton, Florida, USA. p. 1-8.

34. Valberg, S.J., S.S. Lewis, J.L. Shivers, N.E. Barnes, J. Konczak, et al., *The Equine Movement Disorder "Shivers" Is Associated With Selective Cerebellar Purkinje Cell Axonal Degeneration.* Vet Pathol, 2015. **52**(6): p. 1087-98.

35. Aparicio, S.R. and P. Marsden, *A rapid methylene blue-basic fuchsin stain for semi-thin sections of peripheral nerve and other tissues.* J Microsc, 1969B. **89**(1): p. 139-41.

36. Vandevelde, M.H., R.J.; Oevermann, A.;, *Reactions of neurons to injury*, in *Veterinary Neuropathology: Essentials of Theory and Practice*, M.H. Vandevelde, R.J.; Oevermann, A.;, Editor. 2012, Wiley: Bern, Switzerland. p. 14-20.

37. Cashman, C.R. and A. Höke, *Mechanisms of distal axonal degeneration in peripheral neuropathies.* Neurosci Lett, 2015. **596**: p. 33-50.

38. Smith, J.A., B.S. Slusher, K.M. Wozniak, M.H. Farah, G. Smiyun, et al., *Structural Basis for Induction of Peripheral Neuropathy by Microtubule-Targeting Cancer Drugs.* Cancer Res, 2016. **76**(17): p. 5115-23.

39. Toyama, S., N. Shimoyama, H.H. Szeto, P.W. Schiller, and M. Shimoyama, *Protective Effect of a Mitochondria-Targeted Peptide against the Development of Chemotherapy-Induced Peripheral Neuropathy in Mice.* ACS Chem Neurosci, 2018.

40. Feldman, E.L., K.A. Nave, T.S. Jensen, and D.L.H. Bennett, *New Horizons in Diabetic Neuropathy: Mechanisms, Bioenergetics, and Pain.* Neuron, 2017. **93**(6): p. 1296-1313.

41. Malik, R.A., A. Veves, D. Walker, I. Siddique, R.H. Lye, et al., *Sural nerve fibre pathology in diabetic patients with mild neuropathy: relationship to pain, quantitative sensory testing and peripheral nerve electrophysiology.* Acta Neuropathol, 2001. **101**(4): p. 367-74.

42. Jones, G., Y. Zhu, C. Silva, S. Tsutsui, C.A. Pardo, et al., *Peripheral nerve-derived HIV-1 is predominantly CCR5-dependent and causes neuronal degeneration and neuroinflammation.* Virology, 2005. **334**(2): p. 178-93.

43. Hahn, K., B. Robinson, C. Anderson, W. Li, C.A. Pardo, et al., *Differential effects of HIV infected macrophages on dorsal root ganglia neurons and axons.* Exp Neurol, 2008. **210**(1): p. 30-40.

44. Duncan, I.D. and J.P. Hammang, *Ultrastructural observations of organelle accumulation in the equine recurrent laryngeal nerve.* J Neurocytol, 1987. **16**(2): p. 269-80.

45. Cahill, J.I. and B.E. Goulden, *The pathogenesis of equine laryngeal hemiplegia--a review.* N Z Vet J, 1987. **35**(6): p. 82-90.

46. Raff, M.C., A.V. Whitmore, and J.T. Finn, *Axonal self-destruction and neurodegeneration.* Science, 2002. **296**(5569): p. 868-71.

47. Conforti, L., J. Gilley, and M.P. Coleman, *Wallerian degeneration: an emerging axon death pathway linking injury and disease.* Nat Rev Neurosci, 2014. **15**(6): p. 394-409.

48. Gilley, J. and M.P. Coleman, *Endogenous Nmnat2 is an essential survival factor for maintenance of healthy axons.* PLoS Biol, 2010. **8**(1): p. e1000300.

49. Gilley, J., G. Orsomando, I. Nascimento-Ferreira, and M.P. Coleman, *Absence of SARM1 rescues development and survival of NMNAT2-deficient axons.* Cell Rep, 2015. **10**(12): p. 1974-81.

50. Gilley, J., R. Adalbert, G. Yu, and M.P. Coleman, *Rescue of peripheral and CNS axon defects in mice lacking NMNAT2.* J Neurosci, 2013. **33**(33): p. 13410-24.

51. Hicks, A.N., D. Lorenzetti, J. Gilley, B. Lu, K.E. Andersson, et al., *Nicotinamide mononucleotide adenylyltransferase 2 (Nmnat2) regulates axon integrity in the mouse embryo.* PLoS One, 2012.
7(10): p. e47869.

52. Garman, R.H., *Histology of the central nervous system.* Toxicol Pathol, 2011. **39**(1): p. 22-35.

53. Parisi, J.E., H. Mena, and B.W. Scheithauer, *CNS Tumors (excluding pituitary, PNET, and embryonal tumors)*, in *Principles and Practice of Neuropathology*, J.S. Nelson, et al., Editors. 2003, Oxford University Press: New York, USA. p. 298-299.

54. Duncan, I.D., P. Reifenrath, K.F. Jackson, and M. Clayton, *Preferential denervation of the adductor muscles of the equine larynx. II: Nerve pathology.* Equine Vet J, 1991. **23**(2): p. 99-103.

Figure 1 A) Number of cell body profiles in the nucleus ambiguus, in each brainstem region, on the left and right side; B) Mean grouped number of cell body profiles counted within the nucleus ambiguus on the left and right sides of the brainstem with error bars depicting the standard deviation. Despite the mean number of cell body profiles on the left being lower than their right counterparts, the difference did not reach statistical significance ($p=0.28$). Box plots show median, interquartile range and range.

Figure 2 A) Cell bodies of neurons within the left nucleus ambiguus of a horse, sectioned at the obex (H&E). These are typical large, polygonal neurons (black arrow) seen within the nucleus ambiguus with an obvious clear (euchromatic) nucleus containing a prominent, single nucleolus (black dotted arrow). The neuronal cytoplasm has a mildly speckled appearance due to the large number of ribosomes or Nissl's granules present. The surrounding neuropil (blue dotted arrow) contains axons, oligodendrocytes, astrocytes, microglia and vasculature. The small nuclei of oligodendrocytes are scattered throughout the neuropil. Black scale bar = 144μm. B) Cell bodies of neurons in the right nucleus ambiguus at the level of the obex, in the horse (Cresyl Violet). The cytoplasm of the large polygonal cell body profiles stains brightly blue, highlighting Nissl's granules (ribosomes). There is no evidence of chromatolysis in this section. Black scale bar = 137μm.

Figure 3 Luxol Fast Blue staining of the brainstem at a level 8mm rostral to the obex in a horse. Lipoproteins are stained blue, such that areas of demyelination would appear pale. No demyelination was found in this study. The location of the nucleus ambiguus on each side is

highlighted (black circle). The left side of the brainstem is located on the left of the figure. Black scale bar represents 3118μm.

Figure 4 Immunolabelling for GFAP of astrocytes within the nucleus ambiguus of a horse, 4mm rostral to the obex. The two images are of the left (A) and right (B) nucleus ambiguus from the same horse (mild RLN severity), showing the presence of more reactive astrocytes in the right side within this individual horse. The presence of the reactive astrocytes was not accompanied by any signs of neuronal degeneration, nor correlated with RLN severity and so the significance is unknown. Reactive astrocytes were seen with near equal frequency in the left and right nucleus ambiguus, amongst the horses included in this research. The black bar represents 140μm.

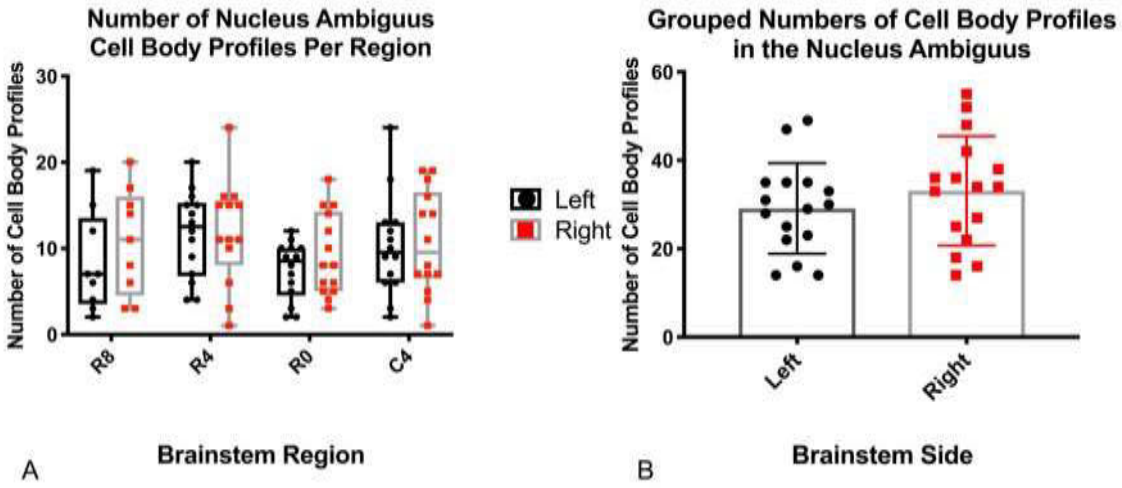
Number of Nucleus Ambiguus
Cell Body Profiles Per Region
Number of Cell Body Profiles
30
20
10
0
R8
R4
R0
C4
Brainstem Region
A
Left
Right
Grouped Numbers of Cell Body Profiles
in the Nucleus Ambiguus
Number of Cell Body Profiles
60
40
20
0
Left
Right
Brainstem Side
B

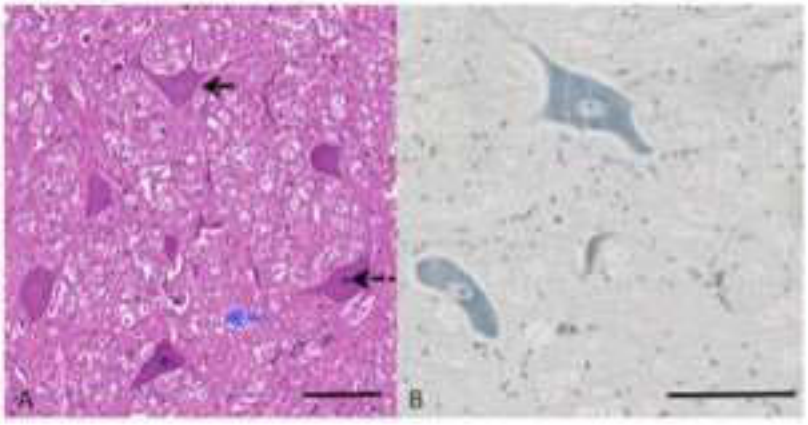
A
B

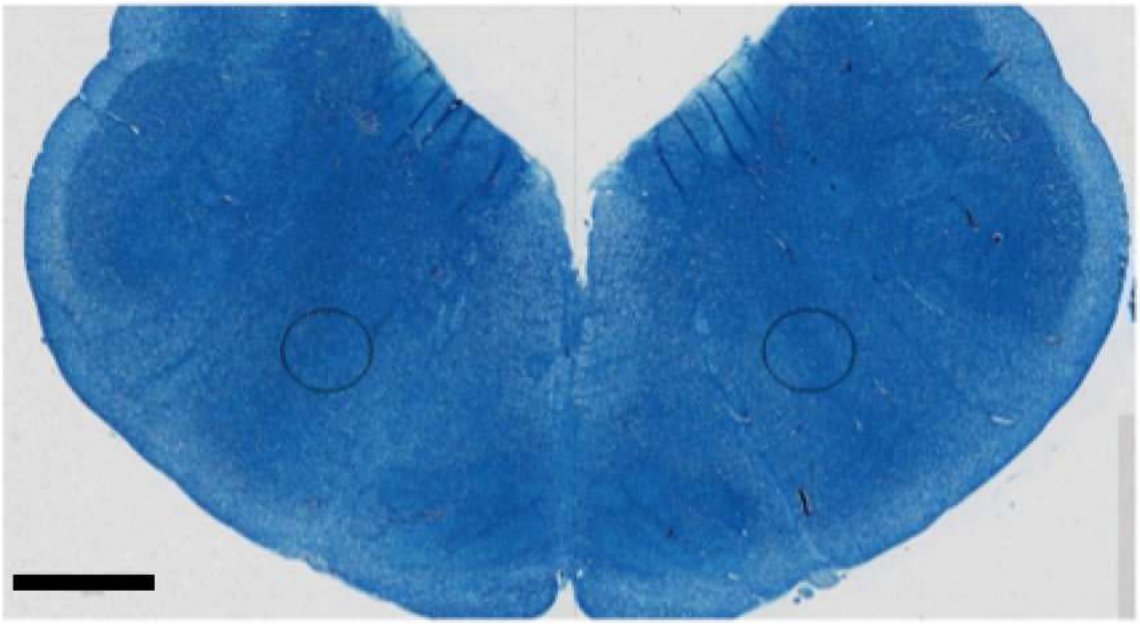

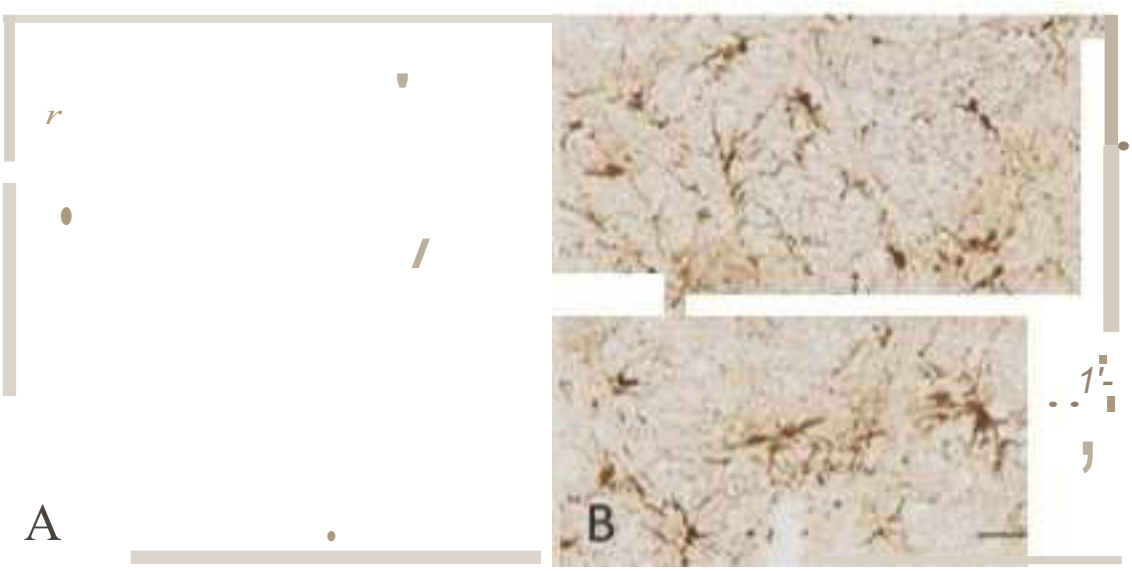
A
B